Design, Fabrication, and Performance Demonstration of a Curvature-Adapted IOnic Eddy Current Testing Probe for WAAM Quality Control

Muhammad Huzaifa Khan Ghory[a], Rameen Khan[1]

[a]*Middle East Technical University, , Ankara, 06800, Cankaya, Turkey*

Abstract

Wire + Arc Additive Manufacturing has, in recent times, proven to be successful for the production of large metal parts. The main drawback of employing WAAM in the industry is that it has no specific quality assurance standards.

A significant contribution to the widespread adoption of WAAM in the industry would be the development of NDT methods tailored to, and integrated within the WAAM process.

To this end, ECT (Eddy Current Testing) can play a significant role, by enabling the inspection of both ferromagnetic and non ferromagnetic materials without contact to the surface. The limitation to commercial ECT is that it can only be utilized to detect surface or sub surface defects.

This study focuses on the development of customized ECT probes according to the geometry of the WAAM weld bead to detect defects significantly below the surface without physical contact.

1. Introduction

Wire arc additive manufacturing (WAAM) is used in the fabrication of large scale metal parts. It is a wire-Direct Energy Deposition (DED) technology in which a metal wire is melted using an arc heat source layer by layer to fabricate the part.

This approach has been rapidly gaining recognition in the industry as a promising manufacturing method. However, the biggest limitation to WAAM as of now is the lack of standardization and reliability. NDT systems designed for and integrated into the WAAM process can accelerate the progression into the mainstream.

The traction AM has gained is largely due to its high deposition rates and efficient material utilization. The variety of materials that can be used for WAAM welding at a low cost also makes it a very attractive choice.

WAAM fabricates components layer by layer forming individual weld beads and then continuing across the specified tool path. This leads to the top layer geometry resembling a bead which is usually at a high temperature. Integrating NDT into such a system is a unique challenge. The geometry of the weld bead and the high temperatures rule out a lot of NDT methods from the get go. One of the methods that can work with this process is Eddy Current Testing (ECT).

ECT is suitable since most of the materials used in WAAM are electrically conductive. This is significant as among the limitations of ECT the chief concern is the material being non conductive. It can be used to inspect both ferromagnetic and non ferromagnetic materials at high speeds and without contact with the test sample surface. However, commercial ECT probes have additional limitations pertaining to the geometry of the inspected components. With regards to WAAM, commercial probes can not efficiently detect cracks or discontinuities within the inspected components. Therefore, further development is required with ECT probes being tailored to the specific geometry of the weld bead.

ECT is an NDT method that is based on the principles of electro-magnetic induction discovered by Micheal Faraday in 1831. Faraday discovered that when an alternating current passes through a coil, it creates a varying magnetic field around the coil. This changing magnetic field will then in turn induce an electro motive force in a conductor that the magnetic field encounters and induce a current in the conductor. The current flowing in the conductor has its own secondary magnetic field which interferes with the primary magnetic field created by the coil. This changes the impedance of the coil if the eddy currents in the conductor encounter a crack or a discontinuity. The theory and application of the induction coils was presented by Maxwell in 1864, and the prediction of the change in impedance of eddy current inspection coils caused by small flaws was done by Hughes in 1879. Finally, the first eddy current instrument used to measure wall thickness was developed by Kranz in the 1920s.

The IOnic probe was invented in 2007 with the goal to increase the capability to detect flaws with sizes or shapes that can not be detected by the conventional probes used in ECT. The key difference between the IOnic probe and the conventional probes is that the IOnic probe consists of a toroidal coil which induces Eddy Currents in multiple directions within the inspected component. This multi directional EC approach suppresses the angular lift off effects of the conventional probes and reduces noise due to the edge effect. Additionally, IOnic probes consist of sensitive coils that are wound in semicircles parallel to the inspected surface and perpendicular to the excitation coil and a support structure that makes up the probe and holds the excitation coil. The sensitive coils on either side of the excita-

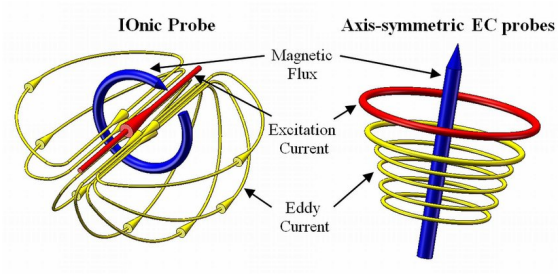

Figure 1: Eddy Currents due to IOnic probes vs conventional pin probes

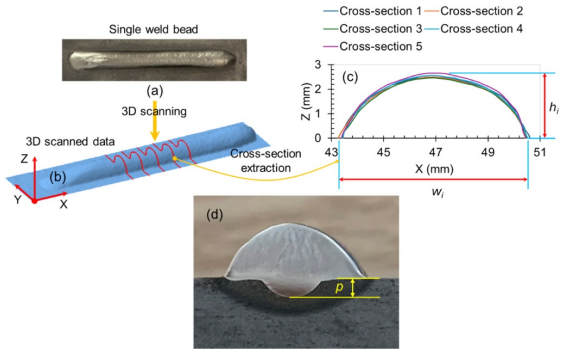

Figure 2: Weld Bead Geometry (a) An example of a deposited WB and (b) its scanned data, (c) the five extracted cross-section curves to measure the width (w) and height (h) of the weld bead, and (d) an image of etched cross-section to measure the penetration depth (p).

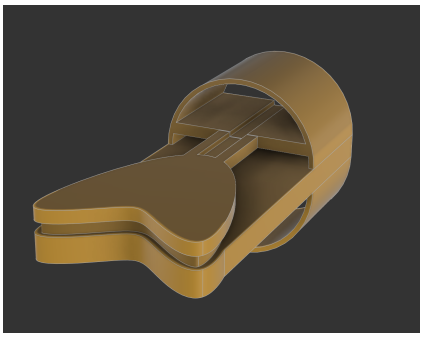

Figure 3: Probe Holder Geometry

tion coil lead to the nullification of the EC on either side. In the case of a crack or discontinuity the impedance of one of the sensitive coils is altered and the defect is detected. This setup, known as a differential probe, is more sensitive than an absolute setup which only detects the perturbation in the impedance of the primary excitation coil.

The goal of this study is to design an ECT probe that :

- Deals with the skin effect by providing a sufficient depth of penetration.
- Reduces the noise due to angular lift off variations caused by the weld geometry.
- Takes into account the high temperatures associated with WAAM and carries out the inspection without contact to the inspected part.

2. WAAM Geometry Analysis and Customization

According to the scope of this study, the parameters examined will be the weld bead width (w), the weld bead height (h), and the penetration depth (p). The data acquired and shown in Figure 1 is obtained from the work of Le et al. (2025) where an analysis of data variation (ANOVA) is applied to observe the effects of process parameters on the geometry of the weld beads. The analysis performed is on an inconel 625 super alloy weld bead. However, as will be discussed later on in the study the variation of parameters is not significantly relevant to our design. The inspected parts the probes in this study are designed for should be applicable to a wide range of WAAM geometries and so the dimensions chosen will account for the variations.

2.1. Weld Bead Geometry

From the work of Le et al. (2025) it is seen that the bead height as shown in Figure 1 monotonically decreases with increasing travel speed speed 'v'. The bead height ranges from 2.97 mm to 4.64 mm. The percentage contribution to the variation of the bead weld height of the travel speed 'v' is 91.31%. Reduced deposition time per unit length at higher levels of 'v' results in less material accumulation, leading to a lower 'h'. The wire feed rate 'wfs' has little to no effect on the weld bead height.

Considering the weld bead width it is observed from the work of Le et al. (2025) that both the travel speed 'v' and wire feed rate 'wfs' have a significant effect. The dominant process parameter in this case is the wire feed rate 'wfs' with a 71.47% contribution to the variation in weld bead width. Reduced heat input per unit length and shorter interaction time between the heat source and the substrate at higher travel speeds. The weld bead width ranges from 5.83 to 8.24 mm.

2.2. Probe Design Customization

This study aims to design an ECT probe that can perform better than a commercialized one. To this end, the chosen design must account for the variations in the weld bead geometry as a result of different process parameters over the board. The chosen design must also take into account the high temperatures associated with WAAM and enable a significant lift off allowance to protect the coils of the probe.

To this end, the bead width was estimated as 7 mm and the bead height as 3 mm from the work of Le et al. (2025). The probe was made thicker overall to increase the separation of the two sensing coils which decreases the overlap and therefore increases the lateral range. Additionally, to facilitate a sufficient air gap and reduce the angular lift off variation an air gap is introduced. This 7 mm diameter air gap facilitates both the bead height and width which reduces angular lift off variations without contact. The sensing coils are also stretched out compared to the reference probe, with the geometry altered to an ellipse. This increases the lateral sensitivity of the coil.

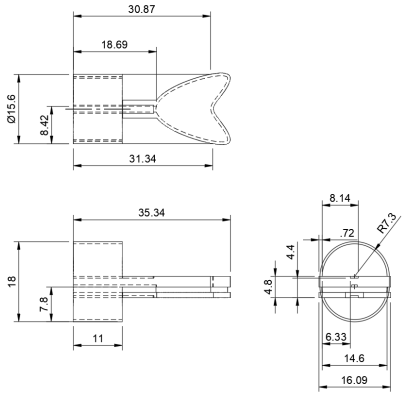

Figure 4: Detailed Drawing with dimensions in mm

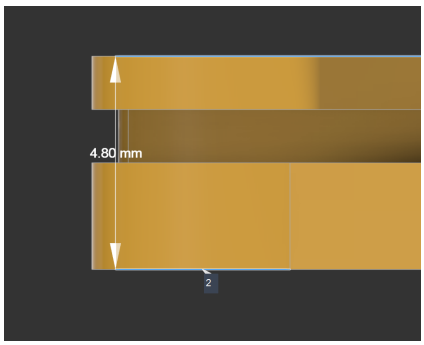

Figure 5: Specified thickness of the probe holder

The probe holder was designed in Siemens NX 11 however there is simplification with regards to the sensing coils. The main distinction is the air gap that is mentioned previously which facilitates the no contact constraint and helps with the angular lift off variations.

3. Sensing Coil Configuration

Three different IOnic probe configurations were taken into consideration as mentioned in detail by Bento et al. (2019).The design features an excitation coil with 100 turns (double the number of turns used in configuration #1) paired with a 20 turn sensitive coil. The justification for this selection is the increased inductance of the excitation coil, which enhances signal penetration depth. The ability of the probe to detect sub-surface level defects (up to 2mm deep) despite the lift off variations (up to 5mm) caused by the surface roughness of the printed layers was prioritized.

3.1. Lift-off Compensation

The selection of configuration #2 addresses the electromagnetic obstacles caused by WAAM production. It is known that the magnetic induction decreases with the square of the distance from the current source. Since the WAAM process involves high temperatures, the probe must maintain a non-contact (lift-off) distance to prevent damage. By increasing the excitation coil winding to 100 turns, Configuration #2 generates a stronger magnetic field to compensate for the lift-off issue. This design ensures that sufficient eddy currents are induced within the aluminum to detect subsurface defects up to 2 mm deep, even when the probe is positioned up to 5 mm away from the material surface.

IOnic Probe	Copper Wire diameter [mm]	No. of Turns Excitation , Sensitive
1	20 * 12 * 12	50 , 20
2	20 * 13 * 14,	100 , 20
3	23 * 12 * 12,	50 , 40

Table 1: IOnic probe configurations

3.2. Numerical Simulation

To support the choice of the IOnic probe over the conventional probe numerical simulation was performed utilizing finite element software. The software used was FEMM and MATLAB was used in post processing.

The simulation was performed by using the primary excitation coil with the support structure removed to simplify the analysis. The main objective of the numerical simulation was to check whether the skin effect could be overcome by the depth of penetration of configuration #2. Copper AWG 18 wire was used as the coil material with the coil having 100 turns. The inspected component was considered as Aluminum, 6061-T6 which has a similar electrical conductivity as the Aluminum used by Bento et al. (2019). A discontinuity is introduced by setting the material as air with no electrical conductivity. This discontinuity measures 0.8 mm by 0.7 mm and is at a 1 mm depth in the aluminum slab.

Considering the high temperatures the WAAM surface reaches during manufacturing a no contact approach is one of the goals of the study which is achieved by setting the lift off to approximately 1 mm.

An Alternating Current with 1 A is passed through the coil at a frequency of 2kHz to achieve a higher penetration depth as is shown by the depth of penetration equation.

Since FEMM is an open source software it comes with a few limitations that are important to discuss. Firstly, the simulation is performed in 2D instead of 3D as is done by Bento et al. (2019) in their research. This is done only considering the fact that the IOnic probe will sufficiently cover the aluminum slab in terms of width, which means that it will induce multidirectional eddy currents through the inspected geometry, although the exact effects could not be observed in this simulation. Secondly, coils can be simplified in by using the axisymmetric problem definition, therefore the test piece is also designed as a ringlike geometry. To address the depth of penetration however this is a sufficient assumption. The results are discussed in the discussion section.

4. Theoretical Eddy Current Testing Analysis

The IOnic probe utilizes a different physics configuration from conventional probes. Its toroidal excitation coil induces

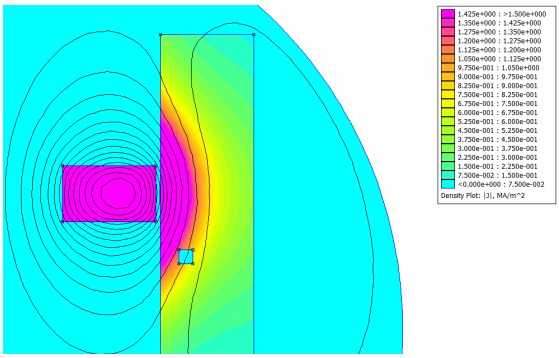

Figure 6: Eddy Current penetration through Aluminum test sample with discontinuity

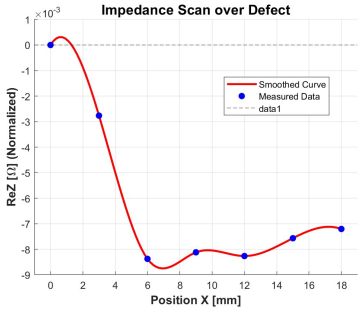

Figure 7: Drop in voltage over discontinuity

multi-directional eddy currents perpendicular to the surface, rather than the standard circular planar currents. The sensing set-up is composed of two planar spiral coils wound in opposite directions, running a differential current. Theoretically, the induced currents in these opposing halves null each other out, resulting in zero potential difference unless a defect disturbs the flow. Regular planar lift-off fluctuations and edge effects do not affect the signals due to this configuration, giving an advantage over conventional probes.

4.1. Skin Effect Mitigation and Penetration Depth

To effectively inspect WAAM components, the system must detect defects beneath the typical 2 mm layer thickness, requiring it overcome the skin effect. The design prioritizes a low operating frequency so that the currents can penetrate deeper into the material. Based on the standard penetration depth equation, a frequency of 2 kHz was selected. Given the high conductivity of the aluminum alloy ($2.63 \cdot 10^7$ S/m), this frequency ensures sufficient standard penetration depth. The calculations below verify the choice that allows eddy currents deep enough to identify subsurface flaws that would otherwise be undetected due to the skin effect.

$$\delta = \frac{1}{\sqrt{\pi f \mu \sigma}}$$

$$\delta = \frac{1}{\sqrt{\pi(2000)(4\pi \times 10^{-7})(2.63 \times 10^{7})}}$$

$$\delta \approx 2.19mm$$

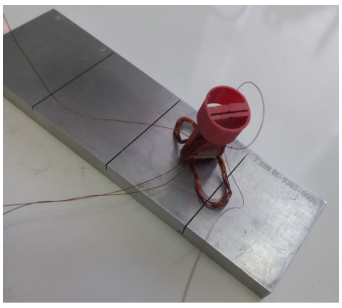

Figure 8: Probe Setup alongside Aluminum Sample

5. Probe Fabrication and Experimental Setup

5.1. Probe Fabrication

Following the design specifications established in Phase 1, the model of the IOnic probe was built using additive manufacturing.The Ender v3 neo was utilized with an 80% infill. The probe core was fabricated using Fused Deposition Modeling (FDM) with Polylactic Acid (PLA) filament, chosen for its non-conductive properties and prototyping ability. The coils were constructed using 0.2 mm diameter enameled copper wire, where the 100-turn excitation coil and the split 20-turn sensitive coils were wound separately before being attached to the core.

5.2. Test Sample Preparation

For experimental validation, the setup utilized Aluminium 2.899.01-9303-0005 samples featuring induced artificial defects, specifically 2 mm deep milled slots, to simulate the surface defects and lack-of-fusion flaws which is a characteristic of the WAAM process.

Additionally, samples of WAAM were also utilized with holes drilled at even spacing 1-2 mm below the surface. The probe in question is designed specifically for no contact with the surface due to the high temperatures of the surface during and after manufacturing. The fabricated probe satisfied this requirement and demonstrated an excellent consistency with the liftoff effect.

5.3. ET Performance Testing

To validate the performance of the fabricated IOnic probe, the experimental data is first compared against the numerical simulation values. Whenever the probe was lifted off the surface, the signal showed a change in the impedance which is consistent. This confirms that the design successfully realised the lift-off effect consistently and returned to the baseline. Furthermore, the probe demonstrated the edge effect, which showed a sharp drop off at the edges of the sample. This is expected due to the differential winding of the sensitive coils since one receives no impedance change due to eddy currents while the other does.

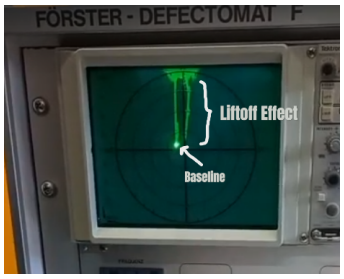

Figure 9: Impedance Graph showing liftoff effect

5.4. Data Analysis and Validation

The probe provided clear and consistent signals for both the lift off and the edge effect, however it was not effective at detecting cracks for the aluminum control blocks. The main reason for this is that the sensitive coils were physically too large in diameter. However, some noise attributed to surface roughness and imperfections in the winding of the coil was observed in the raw signal. Because the sensitive coil diameters were much wider than the tiny slot defects, they "averaged out" the signal over a large area instead of focusing on the small flaw, hence leaving it undetected. To fix this in the future, we would need to wind much smaller sensitive coils to make them sharp enough to spot fine details.

Comparing with commercial probes and Bento et al. (2019) the fabricated probe still requires some crucial changes in order to perform at an industry level. The first and the most critical design change is to reduce the diameter of the sensitive coils, due to the large size of the coverage they pick up impedance changes from a large region defeating the purpose of the differential winding. The other major change that should be implemented in further designs is the number of turns in the sensitive coils. In the fabricated design configuration #2 was chosen from the work of Bento et al. (2019) however this did not provide enough sensitivity. The best case should be to find a balance between the number of turns and the size of the sensing coils which can be implemented in a future design.

6. Discussion

The results of the numerical simulation performed in FEMM are important to consider along with the weld bead geometry and the calculations performed in the theoretical analysis. Figure 4 was obtained by manual iteration of the problem case, shifting the IOnic probe by 3 mm in each iteration until the whole slab was covered. For simplicity the signal is shown at the change in impedance when the discontinuity affects the propagation of Eddy Currents within the material.

From the figure it is apparent that the defect causes a change in the impedance; however during signal processing no phase rotation was applied unlike the reference simulation performed by Bento et al. (2019) which displays a bipolar response. The raw simulation data in this case exhibits a unipolar reduction in resistance which is consistent with the lack of eddy current propagation due to the presence of the discontinuity.

The theoretical analysis determines the depth of penetration around 2 mm which demonstrates the skin effect. The results obtained from the numerical simulation show that the penetration depth of eddy currents is significantly higher. Discontinuities can be detected up to 4 mm deep with a considerable amount of lift off, as is obtained from the numerical analysis in FEMM.

The second phase analysis confirmed that the differential coil configuration effectively stabilizes the signal. The probe showed a clear "signal return" during lift-off and suppressed edge effects better than standard designs, proving the split-coil configuration effectively cancels environmental noise. However, the probe failed to observe fine defects. This is attributed to the sensitive coils being physically larger than the defects, which diluted the signal. While the circuit concept is valid, the current coil size is the primary constraint to successful defect detection.

7. Summary and conclusions

Phase 1 discusses the design framework for a curved IOnic probe for WAAM quality control.Weld bead variations were analyzed initially, where the characteristic height ranged from 2.97–4.64 mm and the widths of 5.83–8.24 mm. Therefore, the support structure is able to satisfy a respectable range of workpieces. For the sensing element, configuration #2 was selected, featuring a 100-turn excitation coil. This choice provided the increased inductance necessary to penetrate the surface despite the significant lift-off allowance (up to 5 mm) required by high temperatures and geometric roughness. Theoretical analysis demonstrated that the probe's differential set-up effectively removes lift-off noise. Finally, an operating frequency of 2 kHz was calculated to overcome the skin effect, achieving a penetration depth of $\approx$ 2.19 mm to inspect the full layer thickness of the component.

Looking ahead, the proposed probe design is optimized for fabrication using Fused Deposition Modeling (FDM) for the customized support structure. While the selected Configuration #2 physically compensates for lift-off, the significant surface roughness identified in the geometric analysis implies that signal noise remains a challenge. Therefore, the upcoming experimental demonstration will require of digital signal processing to further enhance the Signal-to-Noise Ratio (SNR). Ultimately, this theoretical framework provides a solid foundation for achieving the project's objective of quality assurance for aluminum WAAM components.

This project successfully demonstrated that a custom IOnic probe with a differential split-coil design significantly reduces environmental noise, outperforming commercial absolute probes in stability. However, the prototype's sensitivity was limited by the large diameter of the sensitive coils. While the design is effective against lift-off and edge effects, future prototypes must physically minimize the winding process to improve the fill factor and detect micro-scale defects more clearly.

Acknowledgements

This work is largely based off the work done by Bento et al. (2019), and Le et al. (2025) is used as a basis to analyze the Weld bead geometries.

References

Bento, J.B., Lopez, A.B., Pires, I., Quintino, L., Santos, T.G., 2019. Non-destructive testing for wire + arc additive manufacturing of aluminium parts. Additive Manufacturing 29, 100782. doi:10.1016/j.addma.2019.100782.

Le, V.T., Dinh, D.M., Tran, V.C., Muzamil, M., 2025. Modelling, analysis, and multi-objective optimization of single weld bead characteristics in wire arc additive manufacturing of inconel 625 based on machine learning and nsga-ii. Materials Today Communications 49, 113831. doi:10.1016/j.mtcomm.2025.113831.